Adaptive Set-Point Regulation of Linear 2×2 Hyperbolic Systems with Application to the Kick and Loss Problem in Drilling ⋆

Haavard Holta [a], Henrik Anfinsen [a], Ole Morten Aamo [a]

[a] *Department of Engineering Cybernetics. Norwegian University of Science and Technology, Trondheim N-7491, Norway*

Abstract

We study the kick and loss detection and attenuation problem in managed pressure drilling by modeling the well as a distributed parameter system. Two cases are considered, distinguished by whether down-hole pressure measurements are available or not. The main contribution of the paper is a theoretical result on adaptive stabilization and set-point regulation by boundary control for a general 2×2 linear hyperbolic system in the case of measurements taken at both boundaries, with stability proven in the L_2-sense. The design is applied to the drilling system and shown to solve the kick and loss problem with sensing at both boundaries. An earlier result on adaptive set-point regulation for 2×2 hyperbolic systems is also applied to the drilling system and shown to solve a kick and loss problem with sensing restricted to the actuated boundary only. The two designs are compared in a simulation of a loss incident, showing a significant reduction in convergence time and total accumulated loss for the design with sensing allowed at both boundaries.

Key words: Distributed-parameter systems, adaptive control, parameter estimation, managed pressure drilling, kick and loss detection

1 Introduction

1.1 Motivation

A drilling system consists of a drill string with a drill bit at the bottom-hole end and a casing around the drill string called *annulus*. A drilling fluid called *mud* is circulated down the drill string, through the drill-bit and up the annulus to the surface where cuttings are removed and the mud recirculated down the drill string again (see Figure 1). The purpose of the mud is not only to transport the cuttings out of the system, but to provide pressure control throughout the well. If the pressure is too low, the well might collapse, and a too high bottom-hole pressure might lead to fracturing of the formation. Traditionally, pressure is controlled by varying the mud density, viscosity or circulation rate. In *managed pressure drilling* (MPD), with *applied back pressure* (ABP) in particular, the pressure in the annulus is controlled by using a *back pressure valve* top-side to limit the flow and a *back-pressure pump* in the case without circulation. The difficulty in MPD comes from the fact that actuation is located top-side, while the pressure of interest is bottom-hole usually several kilometers away. Sensing is only available at the boundaries and often only top-side.

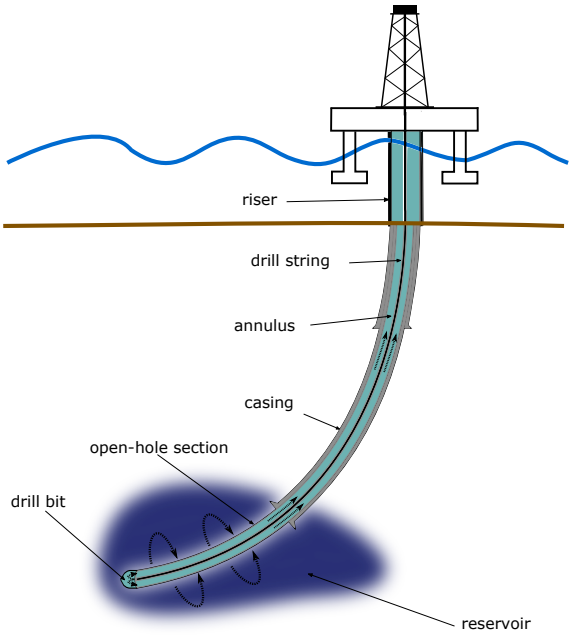

Fig. 1. Schematic of the drilling system.

⋆ Corresponding author: H. Holta. Economic support from The Research Council of Norway and Equinor ASA through project no. 255348/E30 Sensors and models for improved kick/loss detection in drilling (Semi-kidd) is gratefully acknowledged.

Email addresses: haavard.holta@ntnu.no (Haavard Holta), henrik.anfinsen@ntnu.no (Henrik Anfinsen), aamo@ntnu.no (Ole Morten Aamo).

Time spent correcting down-hole errors caused by inadequate pressure control accounts for a significant part of the total non-productive time during drilling [24]. To avoid such errors, it is essential to maintain a down-hole pressure within margins dictated by the surrounding reservoir pressure. When the bottom-hole pressure exceeds the formation pressure drilling mud will flow into the formation, called a *loss*, potentially damaging the well-bore (if exceeding the *fracturing* pressure). A higher formation pressure than down-hole pressure will result in formation fluids flowing into the well, called a *gain* or *kick*. If not handled, a kick leads to formation fluids flowing up the annulus, which in severe circumstances, might lead to uncontrolled blowouts on the surface. Often, a kick is preceded by a loss since the loss causes down-hole pressure to drop. Thus, quick handling of the loss is critical for avoiding a kick incident, which is more serious in terms of safety. Since the reservoir pressure is usually unknown, the challenge is now to stabilize the well pressure, estimate the reservoir pressure and at the same time use this estimate together with well pressure and flow estimates to regulate the bottom-hole pressure.

To model the annular pressure and flow in a well using managed pressure drilling, a modification of the model presented in [22] is used. This model is based on a single mass balance law and a momentum balance linearized around a constant mud density. The model is the result of a trade-off between providing the necessary level of simplicity needed for estimation and control design while at the same time capturing the dominating dynamics in a single-phase system with laminar pipe flow. To model the reservoir relation, the bottom-hole boundary condition is replaced by a simple *productivity index inflow* model where the flow between the reservoir and the well-bore is proportional to the bottom-hole and reservoir pressure difference. This gives the following model:

$$p_t(z,t) = -\frac{\beta}{A} q_z(z,t) \tag{1a}$$

$$q_t(z,t) = -\frac{A}{\rho} p_z(z,t) - \frac{F}{\rho} q(z,t) - Ag\cos\psi(z) \tag{1b}$$

$$q(0,t) = J\left(p_r - p(0,t)\right) + q_{bit} \tag{1c}$$

$$p(l,t) = p_l(t) \tag{1d}$$

where $z \in [0,l]$ and $t \geq 0$ are independent variables of space and time respectively, l is the well depth, $p(z,t)$ is pressure, $q(z,t)$ is volumetric flow, β is the bulk modulus of the mud, ρ is the density of the mud, A is the cross sectional area of the annulus, F is the friction factor, g is the acceleration of gravity, $\psi(z)$ is the angle between the positive flow direction and gravity at position z, $J > 0$ is called the productivity index and is assumed unknown, p_r is the unknown reservoir pressure, and q_{bit} is the known flow through the drill bit. It is assumed that p_r satisfies $0 < p_r \leq \bar{p}_r$ where $\bar{p}_r$ is some known upper bound for the reservoir pressure. Moreover, it is assumed that the choke controller has significantly faster dynamics than the rest of the system so that the actuation dynamics can be ignored and the top-side pressure p_l regarded as a control input. The design goal is to keep the down-hole pressure equal to the unknown reservoir pressure, that is $p(0,t) = p_r$ such that flow between the reservoir and well-bore is zero. This implies that the flow through the annulus is equal to the drill bit flow. Based on the design goal, the control objective

$$\lim_{t\to\infty} \int_t^{t+T} |p_r - p(0,t)|\, d\tau = 0 \tag{2}$$

where $T > 0$ is an arbitrary constant, is selected. To estimate the distributed pressure and flow state and achieve the control objective (2), we assume that the following boundary measurements are available:

- Top-side return flow $q(l,t) =: q_l(t)$.
- Bottom-hole pressure $p(0,t) =: p_0(t)$.

In particular, recent advances in wired-drillpipe technology now provides down-hole pressure in real time, replacing the older less reliable, low bandwidth *mud-pulse*-based pressure measurements.

1.2 Problem statement

The coefficient matrix of (1a) and (1b) (formed by combining the states into vector form and collecting the coefficients of the spatial derivatives into a single matrix) has two distinct, real eigenvalues ($\pm\sqrt{\beta/\rho}$), which shows that (1) is of type *hyperbolic*. For all linear hyperbolic systems, there exists a coordinate transformation transforming the system to *characteristic* form where the coefficient matrix is diagonalized (see e.g. [9]). To ease the control design process and analysis, but also to make the design slightly more general and thereby possibly applicable to other applications, we will in the following study systems in the form

$$u_t(x,t) + \lambda u_x(x,t) = c_1(x)v(x,t) \tag{3a}$$

$$v_t(x,t) - \mu v_x(x,t) = c_2(x)u(x,t) \tag{3b}$$

$$u(0,t) = rv(0,t) + k(\theta - y_0(t)) \tag{3c}$$

$$v(1,t) = \sigma y_1(t) + U(t) \tag{3d}$$

defined for $x \in [0,1]$, $t \geq 0$, where u, v are the system states, $\lambda, \mu > 0$, $c_1(x), c_2(x) \in C([0,1])$ are the source terms, r is a constant and y_0 is a measured signal related to the states by

$$y_0(t) = u(0,t) - b_0 v(0,t) \tag{4}$$

with $b_0 \neq r$. In addition, we have the boundary measurement

$$y_1(t) = u(1,t). \tag{5}$$

The only unknown parameters are $k \in [\underline{k}, \bar{k}] \subset (0,\infty)$ and $\theta \in \mathbb{R}$ where $\underline{k}$ and $\bar{k}$ are known lower and upper bounds on k required for technical reasons in the controller design. In order to select the bounds, we must assume that $r + b_0 k$ is

nonzero with known sign. The control objective (2) can be stated in the new coordinate system as

$$\lim_{t\to\infty}\int_t^{t+T}|\theta - y_0(\tau)|\,d\tau = 0 \tag{6}$$

for some arbitrary $T > 0$.

Remark 1 *Related to system* (1)*, λ and $-\mu$ represent the eigenvalues of the coefficient matrix which is unchanged by the coordinate transformation, the source terms c_1, c_2 account for the frictional loss terms, the unknown parameters J and p_r can be recovered from k and θ, y_0 is related to the down-hole pressure measurement while y_1 is related to the top-side flow measurement, and the parameters r and b_0 are trivially equal to -1 and 1, respectively. The details regarding the diagonalizing change of coordinates from* (1) *to* (3) *can be found in Lemma 5 in Section 3.*

It is assumed that the initial conditions $u(x,0) = u_0(x)$, $v(x,0) = v_0(x)$ satisfy $u_0, v_0 \in \mathscr{B}([0,1])$, where

$$\mathscr{B}([0,1]) = \{f(x) : \sup_{x\in[0,1]} f(x) < \infty\}, \tag{7}$$

in which case it can be shown [30] that (3) has a unique solution that stays in $\mathscr{B}([0,1])$ for all $t \geq 0$ for the form of $U(t)$ used in this paper. The objective is to design a control input $U(t)$ so that system (3) is adaptively stabilized in the L_2-sense and such that the objective (6) is achieved. The structure of this problem, with distributed states, and sensing and actuation only at boundaries, fits perfectly into the control framework of infinite-dimensional backstepping for PDEs. In addition, the unknown parameter part of the problem can be handled by combining the backstepping method with an adaptive parameter update law..

1.3 Previous work

The method of infinite-dimensional backstepping for PDEs was first introduced for parabolic PDEs in [23,27,28], where the gain kernel was expressed as a solution to a well-posed PDE. The first result using backstepping applied on hyperbolic PDEs was for first order systems in [19]. The method was later extended to second order hyperbolic systems in [26], and to two coupled first order hyperbolic systems in [32]. The results in the latter were used in [1] for disturbance attenuation in managed pressure drilling which has similarities to the problem considered in this paper. Disturbance attenuation and trajectory tracking problems based on the internal model principle were further studied in [12,20,21]. Adaptive control of parabolic PDEs is extensively studied in [29]. In recent years, results on adaptive state estimation and closed loop stabilization for hyperbolic PDEs have also emerged. Adaptive observers for $n+1$ hyperbolic systems using sensing collocated with the uncertain boundary parameters can be found in [7] using swapping filters, and in [10] using a Lyapunov approach. The extension to stabilization, without additive boundary parameter, and sensing at the non-actuated boundary restricted to the form $y_0(t) = v(0,t)$, is given in [6]. For systems with non-zero additive terms in the un-actuated boundary, the steady-state *profile* is non-zero. For such systems, we study *boundary set-point regulation*, where the goal is to control the un-actuated boundary to a desired set-point, which is unknown a priori. Adaptive set-point regulation for 2×2 systems with an affine boundary condition is considered in [16] and for a bilinear boundary condition in [15] using a swapping based design. A closed loop controller achieving boundary set-point regulation can be designed by defining a *reference model* and proving stability in terms of a quantity describing the *tracking error*. A model reference adaptive control problem for 2×2 system with a multiplicative boundary condition is studied in [5].

Previous results on kick attenuation in MPD have mainly focused on using lumped drilling models. A lumped ODE model is applied to a gas kick detection and mitigation problem in [33] by using a method for switched control of the bottom-hole pressure. Another lumped model for estimation and control of in-/outflux is presented in [13]. Kick handling methods for a first-order approximation to the PDE system is presented in [2] using LMI (Linear Matrix Inequality) based controller design. In/out-flux detection using an infinite dimensional observer is presented in [14]. Kick handling using a distributed PDE model incorporating a model of the reservoir inflow relation, has to the best of the authors' knowledge not previously been addressed.

1.4 Contributions and paper structure

The contributions in this paper are twofold. First, a theoretical result on adaptive boundary set-point regulation of system (3) achieving (6) and L_2 boundedness of all signals in the closed loop system is derived in Section 2. This is achieved by using some of the ideas on model reference control from [5], but with the additional complexity of having, since the parameter θ is unknown, an unknown set-point (6). Second, both the design from Section 2 and the theoretical results on set-point regulation using only topside sensing from [16] are applied to the kick & loss problem in managed pressure drilling, solving the non-collocated and collocated sensing and control problem, respectively. Feasibility of applying the designs to the MPD model are stated in Corollaries 1 and 2 in Section 3. Finally, the two designs are compared in a simulation study in Section 4, demonstrating the benefit of having down-hole pressure available. The new design (the theoretical design in Section 2 with non-collocated sensing) is a significant improvement over the design for system (3) offered in [15]. The state- and parameter estimation scheme avoids swapping filters, thereby significantly reducing the dynamic order of the controller, the stability analysis is less involved, and performance when applied to the MPD problem is improved.

1.5 Notation

For a signal $z:[0,1]\times[0,\infty)\to\mathbb{R}$, let $||z||=\sqrt{\int_0^1 z^2(x,t)dx}$ denote the L_2-norm. For a time-varying, signal $f(t)$, we use the vector spaces

$$f\in\mathscr{L}_p \leftrightarrow \left(\int_0^\infty |f(t)|^p dt\right)^{\frac{1}{p}}<\infty \tag{8}$$

for $p\geq 1$ with the special case $f\in\mathscr{L}_\infty \leftrightarrow \sup_{t\geq 0}|f(t)|<\infty$. The projection operator Proj is defined as

$$\text{Proj}_{a,b}(\tau,\omega)=\begin{cases}0, & \text{if } \omega=a \text{ and } \tau\leq 0\\ 0, & \text{if } \omega=b \text{ and } \tau\geq 0\\ \tau, & \text{otherwise}\end{cases} \tag{9}$$

2 Control design with non-collocated sensing

2.1 State and parameter estimation

From (4), we see that we can describe the non-actuated boundary in the alternative form

$$u(0,t)=b_0 v(0,t)+y_0(t). \tag{10}$$

Since this form eliminates all unknown parameters from the system, designing an observer estimating the states (u,v) becomes almost trivial. A state observer converging to the true states in finite time is presented in Section 2.1.1. Once the system states are known, we can use boundary condition (3c) to design adaptive laws estimating the unknown parameters. In Section 2.1.2, adaptive laws based on the gradient method for a bilinear parametric model are presented.

2.1.1 Finite-time convergent state observer

Let $\hat{u},\hat{v}$ be the estimates of u,v respectively, and denote the estimation error $\tilde{u}=u-\hat{u}$ and $\tilde{v}=u-\hat{v}$. Choosing the observer

$$\hat{u}_t(x,t)+\lambda\hat{u}_x(x,t)=c_1(x)\hat{v}(x,t)+P_1(x)\tilde{u}(1,t) \tag{11a}$$
$$\hat{v}_t(x,t)-\mu\hat{v}_x(x,t)=c_2(x)\hat{u}(x,t)+P_2(x)\tilde{u}(1,t) \tag{11b}$$
$$\hat{u}(0,t)=b_0\hat{v}(0,t)+y_0(t) \tag{11c}$$
$$\hat{v}(1,t)=\sigma y_1(t)+U(t), \tag{11d}$$

with initial conditions satisfying $\hat{u}(\cdot,0),\hat{v}(\cdot,0)\in\mathscr{B}([0,1])$, gives the error dynamics

$$\tilde{u}_t(x,t)+\lambda\tilde{u}_x(x,t)=c_1(x)\tilde{v}(x,t)-P_1(x)\tilde{u}(1,t) \tag{12a}$$
$$\tilde{v}_t(x,t)-\mu\tilde{v}_x(x,t)=c_2(x)\tilde{u}(x,t)-P_2(x)\tilde{u}(1,t) \tag{12b}$$
$$\tilde{u}(0,t)=b_0\tilde{v}(0,t) \tag{12c}$$
$$\tilde{v}(1,t)=0. \tag{12d}$$

Selecting the injection term P_1,P_2 as $P_1(x)=\lambda P^{uu}(x,1)$, $P_2(x)=\lambda P^{vu}(x,1)$, where (P^{uu},P^{vu}) is the unique solution to a 2×2 hyperbolic system given in [32, Eq. (67)-(74)], and using the invertible backstepping transformation [32, Eq. (60)-(61)], it is possible to show that (12) is equivalent to a system of cascaded transport equations with a zero boundary condition so that $(\tilde{u},\tilde{v})$ will be identically zero for all

$$t\geq t_F:=\lambda^{-1}+\mu^{-1} \tag{13}$$

since the backstepping transformation is invertible.

2.1.2 Parameter estimation

With (u,v) known for all $t\geq t_F$, we can use boundary condition (3c) to define a known signal e as

$$u(0,t)-rv(0,t)=k(\theta-y_0(t))=:e(t) \tag{14}$$

with the corresponding estimate

$$\hat{e}(t):=\hat{k}(t)(\hat{\theta}(t)-y_0(t)). \tag{15}$$

The *gradient method for bilinear parametric models* in [17, Theorem 4.52] can be used to minimize a cost function based on the square error $\tilde{e}^2(t)=(e(t)-\hat{e}(t))^2$ and thereby forming adaptive laws for the parameter estimates $\hat{\theta},\hat{k}$. Parameter projection is employed to force the estimate of k to satisfy the known conditions on k.

Lemma 1 *Consider the adaptive laws*

$$\dot{\hat{\theta}}(t)=\gamma_1\frac{\tilde{e}(t)}{1+y_0^2(t)} \tag{16a}$$
$$\dot{\hat{k}}(t)=\text{Proj}_{\underline{k},\bar{k}}\left(\gamma_2\left[\hat{\theta}(t)-y_0(t)\right]\frac{\tilde{e}(t)}{1+y_0^2(t)},\hat{k}(t)\right) \tag{16b}$$

for $t\geq t_F$ and $\dot{\hat{\theta}}=\dot{\hat{k}}=0$ for $t<t_F$, where $\gamma_1,\gamma_2>0$ is the adaptation gain and where we assume $\underline{k}\leq\hat{k}(0)\leq\bar{k}$. The adaptive laws (16) *have the following properties:*

(1) $\hat{\theta},\hat{k},\in\mathscr{L}_\infty$.
(2) $\underline{k}\leq\hat{k}(t)\leq\bar{k}$ *for all* $t\geq 0$
(3) $\frac{\tilde{e}}{\sqrt{1+y_0^2}}\in\mathscr{L}_2\cap\mathscr{L}_\infty$
(4) $\dot{\hat{\theta}},\dot{\hat{k}},\in\mathscr{L}_\infty\cap\mathscr{L}_2$.
(5) If y_0 *is bounded for* almost all $t\geq 0$ *and* $\hat{\theta}-y_0\in\mathscr{L}_2$, *then* $\hat{\theta}$ *converges to* θ *and* $\hat{k}$ *converges to some constant.*

The proof is given in Appendix A.1.

2.2 Closed loop adaptive controller design

In the following stability analysis, it is more convenient to write boundary condition (3c) in linear form

$$\begin{aligned} u(0,t) =& rv(0,t) + \hat{k}(t)(\hat{\theta}(t) - y_0(t)) + \tilde{e}(t) \\ =& \hat{q}(t)v(0,t) + \hat{d}(t) + \hat{\kappa}(t)\tilde{e}(t) \end{aligned} \tag{17}$$

such that

$$\hat{q}(t) := \frac{r + b_0\hat{k}(t)}{1+\hat{k}(t)}, \hat{d}(t) := \frac{\hat{k}(t)\hat{\theta}(t)}{1+\hat{k}(t)}, \hat{\kappa}(t) := \frac{1}{1+\hat{k}(t)}. \tag{18}$$

To derive a closed loop control law, we use the infinite dimensional backstepping method to stabilize the system by decoupling the state dynamics (3). Since the objective is boundary set-point regulation to an unknown set-point, we design a time varying reference signal and a corresponding reference model we would like our system to track, such that the overall control objective is achieved. To give some intuition behind our selection of control law, we apply a certainty equivalence principle in Section 2.2.1 and propose a control law in Theorem 1. To set the stage for the formal stability proof, which is given in Section 2.3, and to give some further intuition, we use the reference model to derive a final target system that describes the *system tracking error*. Instrumental to the design are the backstepping operators $\mathscr{K}_1, \mathscr{K}_2, \mathscr{K}_{10}, \mathscr{K}_{20} : \mathscr{B}([0,1]) \times \mathscr{B}([0,1]) \to \mathscr{B}([0,1])$ given by

$$\begin{aligned} &\mathscr{K}_1[a,b](x,t) = a(x) - \mathscr{K}_{10}[a,b](x,t) \\ &= a(x) - \int_0^x K^{uu}(x,\xi,t)a(\xi) + K^{uv}(x,\xi,t)b(\xi)d\xi \quad (19a) \\ &\mathscr{K}_2[a,b](x,t) = b(x) - \mathscr{K}_{20}[a,b](x,t) \\ &= b(x) - \int_0^x K^{vu}(x,\xi,t)a(\xi) + K^{vv}(x,\xi,t)b(\xi)d\xi \quad (19b) \end{aligned}$$

where a, $b \in \mathscr{B}([0,1])$, $(K^{uu}, K^{uv}, K^{vu}, K^{vv})$ is the solution to the time-varying system of equations

$$\begin{aligned} K^{uu}_x(x,\xi,t)\lambda + K^{uu}_\xi(x,\xi,t)\lambda =& -K^{uv}(x,\xi,t)c_2(x) \quad (20a) \\ K^{uv}_x(x,\xi,t)\lambda - K^{uv}_\xi(x,\xi,t)\mu =& -K^{uu}(x,\xi,t)c_1(x) \quad (20b) \\ K^{vu}_x(x,\xi,t)\mu - K^{vu}_\xi(x,\xi,t)\lambda =& K^{vv}(x,\xi,t)c_2(x) \quad (20c) \\ K^{vv}_x(x,\xi,t)\mu + K^{vv}_\xi(x,\xi,t)\mu =& K^{vu}(x,\xi,t)c_1(x) \quad (20d) \end{aligned}$$

$$\begin{aligned} K^{uv}(x,x,t)\lambda + K^{uv}(x,x,t)\mu =& c_1(x) \quad (20e) \\ K^{vu}(x,x,t)\lambda + K^{vu}(x,x,t)\mu =& -c_2(x) \quad (20f) \\ K^{uu}(x,0,t)\lambda\hat{q}(t) =& K^{uv}(x,0,t)\mu \quad (20g) \\ K^{vu}(x,0,t)\lambda\hat{q}(t) =& K^{vv}(x,0,t)\mu \quad (20h) \end{aligned}$$

defined over $\{(x,\xi,t) \,|\, 0 \le \xi \le x \le 1, t \ge t_F\}$. From [11], system (20) has a unique, bounded and continuous solution $(K^{uu}, K^{uv}, K^{vu}, K^{vv})$ for any bounded, nonzero $\hat{q}$. Moreover, the mapping $(a,b) \to (\bar{a}, \bar{b})$ given by

$$\begin{aligned} \bar{a}(x) =& \mathscr{K}_1[a,b](x) \\ \bar{b}(x) =& \mathscr{K}_2[a,b](x) \end{aligned} \tag{21}$$

is invertible with unique inverse transformation kernels. In addition, if $\hat{q} \in \mathscr{L}_2 \cap \mathscr{L}_\infty$ then (see [6])

$$||K^{uu}_t||, ||K^{uv}_t||, ||K^{vu}_t||, ||K^{vv}_t|| \in \mathscr{L}_2 \cap \mathscr{L}_\infty. \tag{22}$$

2.2.1 Main result

Let

$$\Psi_1(x,t) := -\lambda K^{uu}(x,0,t) \tag{23a}$$
$$\Psi_2(x,t) := -\lambda K^{uv}(x,0,t). \tag{23b}$$

Furthermore, due to projection of $\hat{k}$ in (16b), $\hat{q}(t)$ given in (18) is bounded. That is

$$|\hat{q}(t)| \le \bar{q} := \max\left| \frac{r + b_0\underline{k}}{1+\underline{k}}, \frac{r+b_0\bar{k}}{1+\bar{k}} \right| \tag{24}$$

for all $t \ge 0$.

Theorem 1 *Let $\bar{\sigma}$ be a known constant such that $|\tilde{\sigma}\bar{q}| < 1, \tilde{\sigma} =: \sigma - \bar{\sigma}$. Consider system* (3) *and the adaptive law* (16)*. The control law*

$$\begin{aligned} U(t) =& \mathscr{K}_{20}[\hat{u},\hat{v}](1,t) - \tilde{\sigma}\mathscr{K}_{10}[\hat{u},\hat{v}](1,t) \\ &+ \frac{1-\tilde{\sigma}r}{r-b_0}\hat{\theta}(t) - \bar{\sigma}y_1(t) \\ &- \hat{d}(t)\int_0^1 (\tilde{\sigma}\lambda^{-1}\Psi_1(\xi,t) + \mu^{-1}\Psi_2(\xi,t))d\xi \end{aligned} \tag{25}$$

guarantees (6)*. Moreover, all signals in the closed loop system are bounded in the L_2-sense, the parameter estimate $\hat{\theta}$ converges to its true value θ and the parameter estimate $\hat{k}$ converges to some constant.*

A schematic of the design showing how the system plant, observer, control law and adaptive law are interconnected is given in Figure 2. Before proving Theorem 1, some intuition behind the selected control law (25) might be clarifying.

Remark 2 *If the parameters (k,θ) are known,we have*

$$q := \frac{r+b_0k}{1+k}, \quad d := \frac{k\theta}{1+k} \tag{26}$$

known, $\tilde{e} = 0$ from (18) *and time-invariant kernels* (20) *and* (23) *(since $q = \hat{q}$ is constant). It is possible to show that*

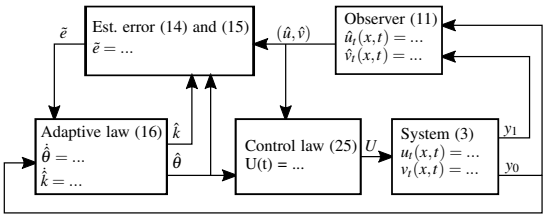

Fig. 2. Structure of the control design.

system (3) *is, through the invertible, time-invariant backstepping transformation* $\bar{\omega}(x,t) = \mathscr{K}_1[u,v](x,t)$ *and* $\bar{\zeta}(x,t) = \mathscr{K}_2[u,v](x,t)$ *for* $t \geq t_F$ *and, by selecting*

$$\begin{aligned} U(t) =& \mathscr{K}_{20}[u,v](1,t) - \tilde{\sigma}\mathscr{K}_{10}[u,v](1,t) \\ &+ \zeta^* - \bar{\sigma} y_1(t), \end{aligned} \tag{27}$$

equivalent to the system of conservation laws

$$\bar{\omega}_t + \lambda\bar{\omega}_x = \Psi_1(x)d \tag{28a}$$
$$\bar{\zeta}_t - \mu\bar{\zeta}_x = \Psi_2(x)d \tag{28b}$$
$$\bar{\omega}(0,t) = q\bar{\zeta}(0,t) + d \tag{28c}$$
$$\bar{\zeta}(1,t) = \tilde{\sigma}\bar{\omega}(1,t) + \zeta^*. \tag{28d}$$

System (28) *is stable for* $|q\tilde{\sigma}| < 1$ *(see [9, Section 2.1]) and the steady state solution* $\bar{\omega}(0,\cdot) = r\bar{\zeta}(0,\cdot)$ *is obtained if* ζ^* *solves*

$$\bar{\omega}(0,\cdot) = r\bar{\zeta}(0,\cdot) \tag{29a}$$
$$\bar{\omega}(0,\cdot) = q\bar{\zeta}(0,\cdot) + d \tag{29b}$$
$$\begin{aligned} \bar{\zeta}(0,\cdot) =& d\int_0^1 (\tilde{\sigma}\lambda^{-1}\Psi_1(\xi) + \mu^{-1}\Psi_2(\xi))d\xi \\ &+ \tilde{\sigma}\bar{\omega}(0,\cdot) + \zeta^*. \end{aligned} \tag{29c}$$

That is, we select

$$\begin{aligned} \zeta^* =& \frac{d(1-\tilde{\sigma}r)}{r-q} - d\int_0^1 (\tilde{\sigma}\lambda^{-1}\Psi_1(\xi) + \mu^{-1}\Psi_2(\xi))d\xi \\ =& \frac{\theta(1-\tilde{\sigma}r)}{r-b_0} - d\int_0^1 (\tilde{\sigma}\lambda^{-1}\Psi_1(\xi) + \mu^{-1}\Psi_2(\xi))d\xi \end{aligned} \tag{30}$$

which resembles (25)*, but with the estimates* $(\hat{u},\hat{v},\hat{\theta})$ *replaced by the true values* (u,v,θ)*. That is, the form of* (25) *is motivated by viewing it as a certainty equivalence design based on* (27) *and* (30)*. If in addition* $\bar{\sigma} = \sigma$*, the system of conservation laws is reduced to a cascaded set of transport equations and we have finite time convergence.*

Remark 3 *It is shown in [8] that complete cancellation of the top-side reflection* σ *by the control law (i.e.* $\bar{\sigma} = \sigma$*) might lead to poor robustness margins in the event of actuator delays. Specifically, it is shown in [8] that systems with* distal reflection θ_1 *(reflection at un-actuated boundary) and* proximal reflection σ *(reflection at the actuated boundary) can not be* delay-robustly stabilized *if* $|\sigma\theta_1| > 1$ *and a control law with complete cancellation is unstable if* $|\sigma\theta_1| > \frac{1}{2}$ *for any non-zero delay. Instead, a control law giving up finite time convergence by preserving a small amount of proximal reflection is proposed and shown to delay-robustly stabilize the system for an arbitrary positive delay and any* $|\sigma\theta_1| < 1$*. Here, the parameter* $\bar{\sigma}$*, in the control law, can be viewed as a design parameter enabling a trade-off between performance and robustness with respect to delays.*

2.3 Stability analysis

Using the backstepping transformation

$$\omega(x,t) = \mathscr{K}_1[u,v](x,t) \tag{31a}$$
$$\zeta(x,t) = \mathscr{K}_2[u,v](x,t), \tag{31b}$$

we get (see [6] for details) the target system

$$\begin{aligned} \omega_t(x,t) =& -\lambda\omega_x(x,t) + \Psi_1(x,t)(\hat{d}(t) + \hat{\kappa}(t)\tilde{e}(t)) \\ &- \int_0^x K_t^{uu}(x,\xi,t)\mathscr{K}_1^{-1}[\omega,\zeta](\xi,t)d\xi \\ &- \int_0^x K_t^{uv}(x,\xi,t)\mathscr{K}_2^{-1}[\omega,\zeta](\xi,t)d\xi \end{aligned} \tag{32a}$$
$$\begin{aligned} \zeta_t(x,t) =& \mu\zeta_x(x,t) + \Psi_2(x,t)(\hat{d}(t) + \hat{\kappa}(t)\tilde{e}(t)) \\ &- \int_0^x K_t^{vu}(x,\xi,t)\mathscr{K}_1^{-1}[\omega,\zeta](\xi,t)d\xi \\ &- \int_0^x K_t^{vv}(x,\xi,t)\mathscr{K}_2^{-1}[\omega,\zeta](\xi,t)d\xi \end{aligned} \tag{32b}$$
$$\omega(0,t) = \hat{q}(t)\zeta(0,t) + \hat{d}(t) + \hat{\kappa}(t)\tilde{e}(t) \tag{32c}$$
$$\begin{aligned} \zeta(1,t) =& \sigma\omega(1,t) + U(t) \\ &+ \sigma\mathscr{K}_{10}[u,v](1,t) - \mathscr{K}_{20}[u,v](1,t). \end{aligned} \tag{32d}$$

Inspired by [5], we define a reference model the target system should track as

$$\varphi_t(x,t) + \lambda\varphi_x(x,t) = \Psi_1(x,t)\hat{d}(t) \tag{33a}$$
$$\phi_t(x,t) - \mu\phi_x(x,t) = \Psi_2(x,t)\hat{d}(t) \tag{33b}$$
$$\varphi(0,t) = \hat{q}(t)\phi(0,t) + \hat{d}(t) \tag{33c}$$
$$\phi(1,t) = \zeta^*(t) + \tilde{\sigma}\varphi(1,t) \tag{33d}$$

with $\varphi(\cdot,0), \phi(\cdot,0) \in \mathscr{B}([0,1])$.

Lemma 2 *Consider the reference model* (33) *with parameter estimates* $(\hat{q},\hat{d})$ *provided by the adaptive laws* (16) *and relations* (18)*. If the tracking signal* ζ^* *is selected as*

$$\begin{aligned} \zeta^*(t) =& \frac{1-\tilde{\sigma}r}{r-\hat{q}(t)}\hat{d}(t) \\ &- \tilde{\sigma}\lambda^{-1}\int_0^1 \Psi_1(\xi,t)\hat{d}(t)d\xi \\ &- \mu^{-1}\int_0^1 \Psi_2(\xi,t)\hat{d}(t)d\xi \end{aligned} \tag{34}$$

and provided $|\tilde{\sigma}\bar{q}| < 1$*, then*

$$(\varphi(0,\cdot,) - r\phi(0,\cdot)) \in \mathscr{L}_2 \cap \mathscr{L}_\infty \tag{35}$$

and

$$||\varphi||, ||\phi|| \in \mathscr{L}_\infty. \tag{36}$$

The proof is given in Appendix A.2.

It now remains to show that the tracking error converges. Defining $\nu = \omega - \varphi$ and $\eta = \zeta - \phi$ and subtracting (33) from (32) and selecting $U(t)$ according to (25) gives the tracking error dynamics

$$\begin{aligned}
\nu_t(x,t) =& -\lambda\nu_x(x,t) + \Psi_1(x,t)\hat{\kappa}(t)\tilde{e}(t) \\
&- \int_0^x K_t^{uu}(x,\xi,t)\mathscr{K}_1^{-1}[\nu+\varphi,\eta+\phi](\xi,t)d\xi \\
&- \int_0^x K_t^{uv}(x,\xi,t)\mathscr{K}_2^{-1}[\nu+\varphi,\eta+\phi](\xi,t)d\xi \quad (37a) \\
\eta_t(x,t) =& \mu\eta_x(x,t) + \Psi_2(x,t)\hat{\kappa}(t)\tilde{e}(t) \\
&- \int_0^x K_t^{vu}(x,\xi,t)\mathscr{K}_1^{-1}[\nu+\varphi,\eta+\phi](\xi,t)d\xi \\
&- \int_0^x K_t^{vv}(x,\xi,t)\mathscr{K}_2^{-1}[\nu+\varphi,\eta+\phi](\xi,t)d\xi \quad (37b) \\
\nu(0,t) =& \hat{q}(t)\eta(0,t) + \hat{\kappa}(t)\tilde{e} \quad (37c) \\
\eta(1,t) =& \tilde{\sigma}\nu(1,t). \quad (37d)
\end{aligned}$$

Our strategy is now to prove stability of the tracking error system (37) (in the L_2-sense), relate this stability result to our original system (3) and show that the objective (6) is achieved. This relationship is studied in Lemma 3 below. Boundedness and convergence to zero in the L_2-sense of the tracking error system (37) is shown in Lemma 4. Finally, these elements are used to prove Theorem 1.

To study the relationship between the tracking error (15) and tracking error dynamics (37), we introduce the auxiliary filter

$$\begin{aligned}
\varpi_t(x,t) - \mu\varpi_x(x,t) =& 0 \quad (38a) \\
\varpi(1,t) =& \nu(0,t) - r\eta(0,t) =: \varpi_1(t) \quad (38b)
\end{aligned}$$

with $\varpi(\cdot,0) \in \mathscr{B}([0,1])$.

Lemma 3 *Assume the properties of Lemma 2 hold. If in addition* $||\varpi|| \in \mathscr{L}_2$*, then*

$$e \in \mathscr{L}_2. \tag{39}$$

If $||\varpi|| \in \mathscr{L}_\infty$*, then e and* y_0 *are bounded a.e.*

The proof is given in Appendix A.3.

Lemma 4 *Consider the tracking error system* (37) *and the filter* (38)*. If*

$$|\tilde{\sigma}\bar{q}| < 1 \tag{40}$$

then we have

$$||\nu||, ||\eta||, ||\varpi|| \in \mathscr{L}_2 \cap \mathscr{L}_\infty \tag{41}$$

and

$$||\nu||, ||\eta||, ||\varpi|| \to 0. \tag{42}$$

The proof is given in Appendix A.4.

We are now ready to prove the main result stated in Theorem 1.

PROOF. [Proof of Theorem 1] By Lemma 4, we have $||\varpi|| \in \mathscr{L}_2$. It then follows from Lemma 3 that $e \in \mathscr{L}_2$ or equivalently $(\theta - y_0) \in \mathscr{L}_2$ which trivially implies (6). Furthermore, since $||\varpi|| \in \mathscr{L}_\infty$ from Lemma 4, we have that ϖ and y_0 are bounded for *almost all* $t \geq 0$. We have

$$\begin{aligned}
\hat{e}(t) \leq& |\varphi(0,t) - r\phi(0,t)| + |\nu(0,t) - r\eta(0,t)| \\
&+ \frac{\tilde{e}(t)}{1+y_0(t)}(1+y_0(t)),
\end{aligned} \tag{43}$$

which by Property 3 in Lemma 1, Lemma 2 and Lemma 3 implies $\hat{e} \in \mathscr{L}_2$. Property 5 in Lemma 1 then gives $\hat{\theta} \to \theta$ and $\hat{k} \to k_\infty$ for some constant k_∞. Lastly for boundedness, combining the results of Lemma 2 and 4 shows boundedness of $||\omega|| \leq ||\nu|| + ||\varphi||$ and $||\zeta|| = ||\eta|| + ||\phi||$ and from the invertibility of the transformations $\omega(x,t) = \mathscr{K}_1[\hat{u},\hat{v}](x,t)$ and $\zeta(x,t) = \mathscr{K}_2[\hat{u},\hat{v}](x,t)$, we have $||u||, ||v|| \in \mathscr{L}_\infty$.

3 Application to the kick & loss problem in MPD

As discussed in the introduction, the motivation for studying the control scheme presented in Section 2 and summarized in Theorem 1 is an application to the kick & loss attenuation problem in MPD where the bottom-hole pressure is measured by utilizing wired-drill-pipe technology. In addition to simplifying state estimation, the bottom-hole measurement facilitates using the bilinear form in (3c) and the bilinear adaptive law which results in strong parameter convergence properties. This section and the next will illustrate the advantage in control performance of utilizing bottom-hole pressure measurements for automatic kick & loss handling. So, in addition to an application of the control scheme in Section 2 (Case 1), we present here the alternative control scheme from [16] only utilizing topside measurements (Case 2).

Case 1 *The* non-collocated *case assumes that both the top-side flow* $q(l,t) = q_l(t)$ *and the down-hole pressure* $p(0,t)$ *are measured. Lemma 5 (see below) ensures that system* (1) *with the specified measurements and control objective* (2) *is equivalent to system* (3) *with measurements* (4) *and* (5) *and control objective* (6)*, and provides in explicit form the coordinate transformation.*

Case 2 *The* collocated *sensing and control case assumes only top side flow $q(l,t)=q_l(t)$ is measured. Since the down-hole pressure measurement is unavailable in this case, it is more convenient to write the boundary condition in affine form, giving the system equations*

$$u_t(x,t)+\lambda u_x(x,t)=c_1(x)v(x,t) \tag{44a}$$
$$v_t(x,t)-\mu v_x(x,t)=c_2(x)u(x,t) \tag{44b}$$
$$u(0,t)=\theta_1 v(0,t)+\theta_2 \tag{44c}$$
$$v(1,t)=\sigma y_1(t)+U(t) \tag{44d}$$

where u,v,λ,μ,c_1,c_2 are defined as in the non-collocated case, θ_1 and θ_2 are the unknown boundary parameters and $u(\cdot,0)$, $v(\cdot,0)\in\mathscr{B}([0,1])$. The only measurement is $u(1,t)=y_1(t)$ and the control objective (2) *can be stated in the new coordinate system as*

$$\lim_{t\to\infty}\int_t^{t+T}|u(0,t)-rv(0,t)|\,d\tau=0 \tag{45}$$

for some arbitrary $T>0$ where $r\neq\theta_1$. As for Case 1, Lemma 5 provides equivalence between systems (1) *and* (44) *for Case 2.*

Lemma 5 *The coordinate transformation*

$$u(x,t)=\frac{1}{2}\left(\frac{A}{\sqrt{\beta\rho}}\left(p(xl,t)+\rho g\int_0^{xl}\cos\psi(s)ds+\frac{F}{A}q_{bit}lx\right)+q(xl,t)-q_{bit}\right)\exp(\frac{lF}{2\sqrt{\beta\rho}}x) \tag{46a}$$
$$v(x,t)=\frac{1}{2}\left(-\frac{A}{\sqrt{\beta\rho}}\left(p(xl,t)+\rho g\int_0^{xl}\cos\psi(s)ds+\frac{F}{A}q_{bit}lx\right)+q(xl,t)-q_{bit}\right)\exp(-\frac{lF}{2\sqrt{\beta\rho}}x) \tag{46b}$$

where

$$x=\frac{z}{l} \tag{47}$$

maps system (1) *into the forms* (3) *and* (44) *with*

$$\lambda=\mu=\sqrt{\frac{\beta}{\rho}}\frac{1}{l} \tag{48a}$$
$$c_1(x)=c_2(-x)=-\frac{F}{2\rho}\exp(\frac{lF}{\sqrt{\beta\rho}}x) \tag{48b}$$
$$\theta_1=\frac{\left(J\frac{\sqrt{\beta\rho}}{A}-1\right)}{\left(J\frac{\sqrt{\beta\rho}}{A}+1\right)},\quad \theta_2=\frac{J}{\left(J\frac{\sqrt{\beta\rho}}{A}+1\right)}p_r \tag{48c}$$
$$k=J\frac{\sqrt{\beta\rho}}{A},\quad \theta=\frac{A}{\sqrt{\beta\rho}}p_r \tag{48d}$$
$$\sigma=\exp(-\frac{lF}{\sqrt{\beta\rho}}). \tag{48e}$$

and

$$U(t)=-\frac{A}{\sqrt{\beta\rho}}\left(p(l,t)+\rho g\int_0^l\cos\psi(s)ds+\frac{F}{A}q_{bit}l\right)\times\exp(-\frac{lF}{2\sqrt{\beta\rho}}) \tag{49a}$$
$$y_1(t)=\frac{1}{2}\left(\frac{A}{\sqrt{\beta\rho}}\left(p(l,t)+\rho g\int_0^l\cos\psi(s)ds+\frac{F}{A}q_{bit}l\right)+q(l,t)-q_{bit}\right)\exp(-\frac{lF}{2\sqrt{\beta\rho}}) \tag{49b}$$
$$y_0(t)=\frac{A}{\sqrt{\beta\rho}}p_0(t). \tag{49c}$$

The measurement y_0 is related to (u,v) by

$$y_0(t)=u(0,t)-v(0,t) \tag{50}$$

implying $b_0=1$. Moreover, the control objective (2) *is transformed to* (6) *or* (45) *with $r=-1$.*

PROOF. The constant terms are removed and the origin shifted by defining

$$\bar{p}(z,t)=p(z,t)+\rho g\int_0^z\cos\psi(s)ds+\frac{F}{A}q_{bit}z \tag{51a}$$
$$\bar{q}(z,t)=q(z,t)-q_{bit}. \tag{51b}$$

Next, introducing the diagonalizing change of variables

$$\bar{u}(z,t)=\frac{1}{2}\left(\bar{q}(z,t)+\frac{A}{\sqrt{\beta\rho}}\bar{p}(z,t)\right) \tag{52a}$$
$$\bar{v}(z,t)=\frac{1}{2}\left(\bar{q}(z,t)-\frac{A}{\sqrt{\beta\rho}}\bar{p}(z,t)\right), \tag{52b}$$

the following relations can be found:

$$\bar{u}(z,t)+\bar{v}(z,t)=\frac{1}{2}\left(\bar{q}(z,t)+\frac{A}{\sqrt{\beta\rho}}\bar{p}(z,t)\right)+\frac{1}{2}\left(\bar{q}(z,t)-\frac{A}{\sqrt{\beta\rho}}\bar{p}(z,t)\right)=\bar{q}(z,t) \tag{53}$$

and

$$\frac{\sqrt{\beta\rho}}{A}\left(\bar{u}(z,t)-\bar{v}(z,t)\right)=\frac{\sqrt{\beta\rho}}{2A}\left(\bar{q}(z,t)+\frac{A}{\sqrt{\beta\rho}}\bar{p}(z,t)\right)-\frac{\sqrt{\beta\rho}}{2A}\left(\bar{q}(z,t)-\frac{A}{\sqrt{\beta\rho}}\bar{p}(z,t)\right)=\bar{p}(z,t). \tag{54}$$

Evaluating (51b) at $z = 0$ gives

$$\begin{aligned}\bar{q}(0,t) &= q(0,t) - q_{bit} \\ &= J\left(p_r - p(0,t)\right) + q_{bit} - q_{bit} \\ &= -J\bar{p}(0,t) + Jp_r,\end{aligned} \tag{55}$$

inserting the relations (53) and (54) yield

$$\begin{aligned}\bar{u}(0,t) + \bar{v}(0,t) &= \bar{q}(0,t) \\ &= -J\bar{p}(0,t) + Jp_r \\ &= -J\frac{\sqrt{\beta\rho}}{A}\left(\bar{u}(0,t) - \bar{v}(0,t)\right) + Jp_r\end{aligned} \tag{56}$$

and by reorganizing the terms and using definitions (48c), one obtains (44c). Evaluating (46a) and (46b) at $x = 0$ and adding them together yield

$$\begin{aligned}u(0,t) + v(0,t) =& q(0,t) - q_{bit} = J\left(p_r - p(0,t)\right) \\ =& J\frac{\sqrt{\beta\rho}}{A}\left(\frac{A}{\sqrt{\beta\rho}}p_r - \frac{A}{\sqrt{\beta\rho}}p(0,t)\right)\end{aligned} \tag{57}$$

and the boundary condition (3c) is obtained with θ and k given in (48d). Subtracting (46a) evaluated at $x = 0$ from (46b) evaluated at $x = 0$ gives

$$u(0,t) - v(0,t) = \frac{A}{\sqrt{\beta\rho}}p(0,t) \tag{58}$$

and the measurement (4) is obtained with y_0 given by (49c) and $b_0 = 1$. From (57), it can be seen that $p(0,t) = p_r$ corresponds to $u(0,t) + v(0,t) = 0$ and the objective (2) is transformed to (6) or (45) with $r = -1$. The rest of the proof is similar to the proof of [1, Lemma 10] and therefore omitted.

From (48c) and the fact that $J > 0$, it can be seen that θ_1 satisfies

$$-1 < \theta_1 < 1 \tag{59}$$

which together with $r = -1$ means that the constraint $r \notin [\underline{\theta}_1, \bar{\theta}_1]$ in [16] is satisfied. Inequality (59) can also be used as lower and upper bounds for θ_1. Lower and upper bounds for θ_2 can be found by using that $0 < p_r < \bar{p}_r$ as $\underline{\theta}_2 = 0$ and $\bar{\theta}_2 = \bar{p}_r$ respectively. From (48d) and $J > 0$, we have that $\text{sign}(k)$ is known and positive. The bounds $[\underline{k}, \bar{k}]$ will depend on the specific well considered. Furthermore, it can be seen that the selected b_0 and r satisfy the constraint $r \neq b_0$.

Corollary 1 (Non-collocated sensing and control) *Consider the system* (1)*. Let $\hat{J}$ and $\hat{p}_r$ be the estimates of the unknown system parameters J and p_r generated using the adaptive law in Lemma 1 and definition* (48d)*. If the system parameters and r are selected according to Lemma 5, the control law*

$$p_l(t) = \frac{\sqrt{\beta\rho}}{A}U(t)\sigma^{-\frac{1}{2}} - \rho g\int_0^l \cos\psi(s)ds - \frac{F}{A}q_{bit}l \tag{60}$$

with $U(t)$ given by (25)*, guarantees* (2) *and that all signals in the closed loop system are bounded. Moreover, the estimate $\hat{p}_r$ converges to its true value p_r in the sense*

$$\hat{p}_r(t) \to p_r. \tag{61}$$

PROOF. For the first part, it suffices to show that the actuation $p_l(t)$ is related to $U(t)$ through (60), since it is established in Lemma 5 that the system (1) takes the form (3). Solving (49a) for $p(xl,t)$ gives trivially the control law (60). By Theorem 1, the control objective (2) is achieved for some $T > 0$ and all signals in the closed loop are bounded. Convergence in $\hat{p}_r$ follows directly from the definition (48d) and convergence in $\hat{\theta}$ to θ from Theorem 1.

Corollary 2 (Collocated sensing and control) *Consider the system* (1)*. Let $(\hat{p},\hat{q})$ be estimates of the states (p,q) generated from the observer in [16] and transformation* (46)*, and let $\hat{J}$ and $\hat{p}_r$ be estimates of the unknown system parameters J and p_r generated using the adaptive law in [16] and definition* (48c)*. If the system parameters and r are selected according to Lemma 5, the control law*

$$p_l(t) = \frac{\sqrt{\beta\rho}}{A}U(t)\sigma^{-\frac{1}{2}} - \rho g\int_0^l \cos\psi(s)ds - \frac{F}{A}q_{bit}l \tag{62}$$

with $U(t)$ given by the control law in [16], guarantees (2) *and all signals in the closed loop system are bounded. Moreover, the estimate $\hat{p}_r$ converges to its true value p_r in the sense*

$$\int_t^{t+T} |\hat{p}_r(\tau) - p_r|\, d\tau \to 0. \tag{63}$$

PROOF. For the first part, it suffices to show that the actuation $p_l(t)$ is related to $U(t)$ through (62), since it is established in Lemma 5 that system (1) takes the form (3) with boundary condition (44c). Solving (49a) for $p(xl,t)$ and evaluating the resulting equation at $x = 1$ give trivially the control law (62). By the control law in [16, Theorem 2], the control objective (2) is achieved for some $T > 0$ and all signals in the closed loop are bounded, furthermore it follows that

$$\int_t^{t+T} |\hat{p}(0,\tau) - p(0,\tau)|\, d\tau \to 0 \tag{64}$$

and since the control objective (2) is satisfied, we obtain (63).

Remark 4 *Comparing the designs presented in Corollaries 1 and 2, we see that when a down-hole pressure measurement is available, it is possible to estimate both the pressure and flow distribution in the well in finite time. The collocated design with only top-side flow measurement on the other hand, achieves only asymptotically converging pressure and flow estimates. Furthermore, with non-collocated control and sensing we are able to prove convergence in the*

reservoir pressure in the strong sense (61). *The greatest advantage of using the non-collocated design, however, is the total convergence time of the overall control objective* (2). *This will be apparent in the next section.*

Remark 5 *In reality, the top-side pressure and flow are related through a choke equation (see eg. [25]). As mentioned in the introduction, we avoid this dynamic by assuming that the top-side pressure is directly controllable. As mentioned in Remark 3, complete cancellation of top-side reflection might lead to instabilities in the event of time delays introduced by the choke actuation system.*

For a typical set of drilling parameters and productivity indices J in the range $[1,385]$ $bbl/psi/day$, as reported by [4], it can be shown that $|\sigma\theta_1| < \frac{1}{2}$ is usually satisfied. Nonetheless, very large and very small J might fall outside this region. In those cases, using $\bar{\sigma} \neq \sigma$ satisfying $|\sigma - \bar{\sigma}| < 1$ might yield sufficient delay-robustness. A rigorous analysis of the control design in these rare cases is however outside the scope of this paper. In the simulation in the next section, the parameters fall within the region where $|\sigma\theta_1| < \frac{1}{2}$ and we set $\bar{\sigma} = \sigma$.

4 Simulation

Although both methods can be applied to both a kick handling problem and a loss handling handling problem. The original model (1) is based on a single-phase assumption. Even though liquid kicks (oil and water) will introduce new phases of matter into the system in addition to the mud phase (and rock cuttings), the model (1) is still a reasonable approximation as all liquid phases can effectively be lumped into a single liquid phase [3]. Gas kick on the other hand can not accurately be modeled by (1). Of the two, gas kicks is by far the most challenging. For this reason, we will in the following study a loss scenario where the only circulating matter is the drilling mud (in addition to rock cuttings) and the single-phase assumption is satisfied.

Both the control scheme for non-collocated sensing and control (the non-collocated method) developed in this paper and the scheme for collocated sensing and control (the collocated method) presented in [16] are implemented in MATLAB and applied to the loss problem in MPD. For the non-collocated method, the implemented system consists of the adaptive law of Lemma 1, and the control law (25). For the collocated method, the observer, adaptive law and control law from Theorem 1 and 2 in [16] are implemented. The system parameters are chosen as

$$\begin{aligned}
\beta &= 7317 \times 10^5 \,\mathrm{Pa} && \text{(65a)}\\
\rho &= 1250 \,\mathrm{kg\,m^{-3}} && \text{(65b)}\\
l &= 2500 \,\mathrm{m} && \text{(65c)}\\
A &= 0.024 \,\mathrm{m^2} && \text{(65d)}\\
F &= 50 \,\mathrm{kg\,m^{-3}} && \text{(65e)}\\
g &= 9.81 \,\mathrm{m\,s^{-2}} && \text{(65f)}\\
q_{bit} &= 0.1 \,\mathrm{m^3\,s^{-1}} && \text{(65g)}\\
J &= 1.068 \times 10^{-8} \,\mathrm{m^3\,s^{-1}\,Pa^{-1}} && \text{(65h)}\\
\psi(z) &= 0 \quad \forall z \in [0,l]. && \text{(65i)}
\end{aligned}$$

The reservoir pressure is initially set to $p_r(0) = 450\,\mathrm{bar}$ and kept constant until a step to $p_r(t \geq t_0) = 400\,\mathrm{bar}$ occurs at $t_0 = 10\,\mathrm{s}$. The system is at steady state at $t = 0$ with the initial bottom-hole pressure set equal to the reservoir pressure and the bottom-hole flow equal to the drill bit flow. This is the typical scenario of drilling ahead into an unforeseen low-pressure pocket in the reservoir, causing a loss of circulation fluid into the formation. The adaptation gains are selected as $\gamma_1 = \gamma_2 = 5$. From (48d) we find that $k \approx 0.4$ and we use the projection bounds $[\underline{k}, \bar{k}] = [k_0, 1 - k_0]$ with $k_0 = 0.01$.

Figures 3 and 4 compare the bottom-hole pressure and flow when using the two methods. The methods are also compared to a simple control method (the simple method) where the top-side flow is kept equal to the drill bit flow $q(l,t) = q_{bit}$. The figures show that all three methods are able to attenuate the mud loss. The bottom-hole pressure is stabilized at the reservoir pressure and the net loss out of the well converge to zero. It is seen that both the collocated and non-collocated method are significantly faster than the simple method. Figure 10 shows that the collocated method offers a $\sim 40\%$ reduction in accumulated out-flow over the simple method, and the non-collocated an additional $\sim 45\%$ reduction over the collocated method. As can be seen in Figures 5 and 6, this is due to the much faster, finite time convergent observer in the non-collocated design. Figure 9 compares the control input, in terms of controlled top-side pressure. It is clear that the non-collocated controller reacts much quicker than the two other methods. Furthermore, we observe in Figures 7 and 8 that in both designs, the reservoir pressure estimate converges to the true reservoir pressure and the productivity index to some constant.

The non-collocated method also has some implementational advantages over the collocated method: The backstepping kernels used in the collocated observer are time-varying and must therefore be solved on-line. In contrast, the injection terms used in (11) are static and can be solved off-line, yielding a much more computationally efficient observer. Both methods, however, require time-varying controller kernels which must be solved on-line.

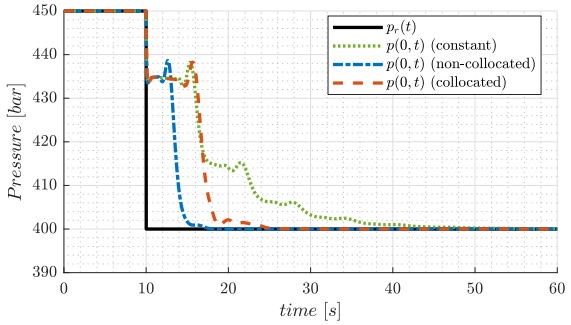

Fig. 3. Bottom-hole pressure.

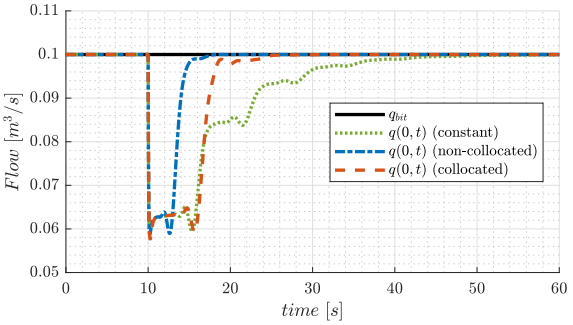

Fig. 4. Bottom-hole flow.

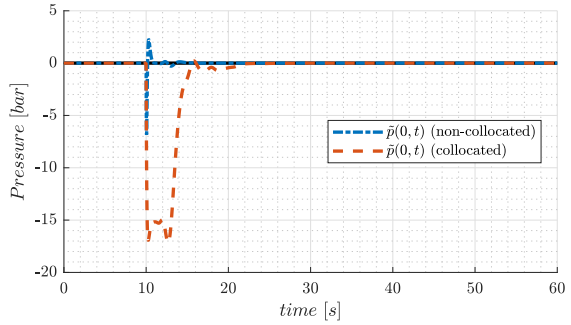

Fig. 5. Bottom-hole pressure estimation error.

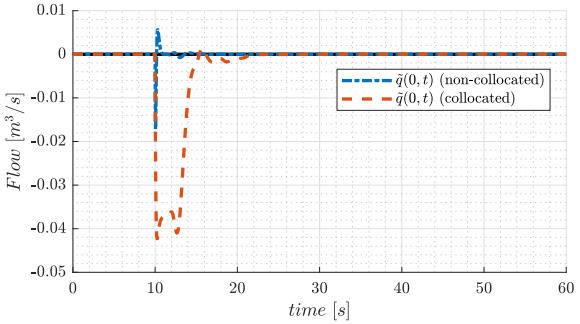

Fig. 6. Bottom-hole flow estimation error.

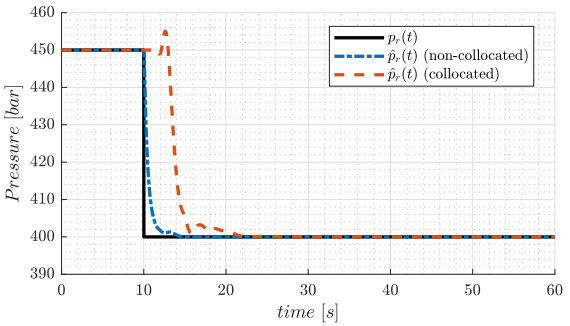

Fig. 7. Reservoir pressure estimate.

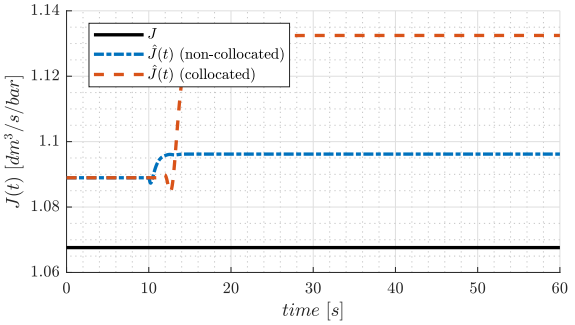

Fig. 8. Productivity index estimate.

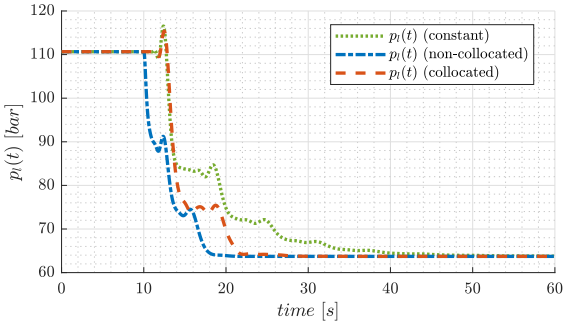

Fig. 9. Control input signal.

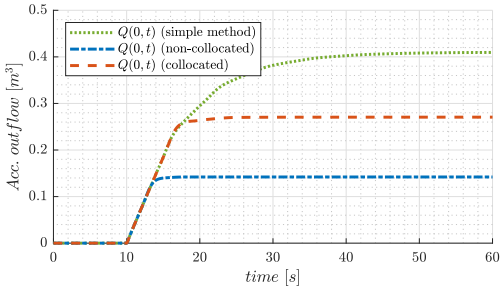

Fig. 10. Accumulated net outflow.

5 Concluding Remarks

We have studied set-point regulation of a 2×2 hyperbolic system with unknown boundary parameters appearing in a special bilinear form. Measurements at both boundaries allowed us to design a finite-time convergent state observer, which in turn was used to design adaptive laws based on a bilinear parametric model. Properties regarding parameter convergence were utilized to design a control law that achieves boundary set-point regulation. The theory was applied to the kick & loss attenuation problem in MPD and compared to an earlier result on stabilization of the same type of system utilizing only top-side sensing. Significant performance improvements was demonstrated for the method utilizing bottom-hole pressure measurements, both in terms of total convergence time and computational complexity, and most importantly in terms of total loss size.

References

[1] Ole Morten Aamo. Disturbance rejection in 2×2 linear hyperbolic systems. *IEEE Transactions on Automatic Control*, 58(5):1095–1106, 2013.

[2] Ulf Jakob F Aarsnes, Behçet Açıkmeşe, Adrian Ambrus, and Ole Morten Aamo. Robust controller design for automated kick handling in managed pressure drilling. *Journal of Process Control*, 47:46–57, 2016.

[3] Ulf Jakob F. Aarsnes, Florent Di Meglio, and Steinar Evje. Control-oriented drift-flux modeling of single and two-phase flow for drilling. In *ASME 2014 Dynamic Systems and Control Conference*, October 2014.

[4] Sulaiman Alarifi, Sami AlNuaim, and Abdulazeez Abdulraheem. Productivity index prediction for oil horizontal wells using different artificial intelligence techniques. In *SPE Middle East Oil & Gas Show and Conference*. Society of Petroleum Engineers, 2015.

[5] Henrik Anfinsen and Ole Moren Aamo. Model reference adaptive control of2×2coupled linear hyperbolic PDEs. *IEEE Transactions on Automatic Control*, 63(8):2405–2420, Aug 2018.

[6] Henrik Anfinsen and Ole Morten Aamo. Adaptive stabilization of $n+1$ coupled linear hyperbolic systems with uncertain boundary parameters using boundary sensing. *Systems & Control Letters*, 99:72–84, 2017.

[7] Henrik Anfinsen, Mamadou Diagne, Ole Moren Aamo, and Miroslav Krstic. An adaptive observer design for $n+1$ coupled linear hyperbolic PDEs based on swapping. *IEEE Transactions on Automatic Control*, 61(12):3979–3990, December 2016.

[8] Jean Auriol, Ulf Jakob Flo Aarsnes, Philippe Martin, and Florent Di Meglio. Delay-robust control design for two heterodirectional linear coupled hyperbolic PDEs. *IEEE Transactions on Automatic Control*, 63(10):3551–3557, oct 2018.

[9] Georges Bastin and Jean-Michel Coron. *Stability and boundary stabilization of 1-D hyperbolic systems*, volume 88. Springer, 2016.

[10] Michelangelo Bin and Florent Di Meglio. Boundary estimation of parameters for linear hyperbolic PDEs. *IEEE Transactions on Automatic Control*, 62(8):3890–3904, Aug 2017.

[11] Jean-Michel Coron, Rafael Vazquez, Miroslav Krstic, , and Georges Bastin. Local exponential H^2 stabilization of a 2×2 quasilinear hyperbolic system using backstepping. *SIAM Journal on Control and Optimization*, 51(3):2005–2035, 2013.

[12] Joachim Deutscher. Finite-time output regulation for linear 2×2 hyperbolic systems using backstepping. *Automatica*, 75:54–62, 2017.

[13] Espen Hauge, Ole Morten Aamo, and John-Morten Godhavn. Model-based estimation and control of in/out-flux during drilling. In *Proceeding of the 2012 American Control Conference*, pages 4909–4914. IEEE, 2012.

[14] Espen Hauge, Ole Morten Aamo, and John-Morten Godhavn. Application of an infinite-dimensional observer for drilling systems incorporating kick and loss detection. In *Proceedings of the 12th European Control Conference*, pages 1065–1070. IEEE, 2013.

[15] Haavard Holta and Ole Morten Aamo. Boundary set-point regulation of a linear 2×2 hyperbolic PDE with uncertain bilinear boundary condition. In *2018 IEEE Conference on Decision and Control (CDC)*. IEEE, dec 2018.

[16] Haavard Holta, Henrik Anfinsen, and Ole Morten Aamo. Adaptive set-point regulation of linear 2×2 hyperbolic systems with uncertain affine boundary condition using collocated sensing and control. In *Proceeding of the 2017 Asian Control Conference*, pages 2766–2771, Dec 2017.

[17] Petros A Ioannou and Jing Sun. *Robust Adaptive Control*. Courier Corporation, 2012.

[18] Miroslav Krstic, Ioannis Kanellakopoulos, and Peter V Kokotovic. *Nonlinear and Adaptive Control Design*. Wiley, 1995.

[19] Miroslav Krstic and Andrey Smyshlyaev. Backstepping boundary control for first-order hyperbolic PDEs and application to systems with actuator and sensor delays. *Systems & Control Letters*, 57(9):750 – 758, 2008.

[20] Pierre-Olivier Lamare and Nikolaos Bekiaris-Liberis. Control of 2×2 linear hyperbolic systems: Backstepping-based trajectory generation and PI-based tracking. *Systems & Control Letters*, 86:24–33, 2015.

[21] Pierre-Olivier Lamare and Florent Di Meglio. Adding an integrator to backstepping: Output disturbances rejection for linear hyperbolic systems. In *2016 American Control Conference*. IEEE, July 2016.

[22] Ingar Skyberg Landet, Alexey Pavlov, and Ole Morten Aamo. Modeling and control of heave-induced pressure fluctuations in managed pressure drilling. *IEEE Transactions on Control Systems Technology*, 21(4):1340–1351, 2013.

[23] Weijiu Liu. Boundary feedback stabilization of an unstable heat equation. *SIAM Journal on Control and Optimization*, 42(3):1033–1043, 2003.

[24] Rystad Energy. New horizon in the deep watermarket, 2014.

[25] R.B. Schller, T. Solbakken, and S. Selmer-Olsen. Evaluation of multiphase flow rate models for chokes under subcritical oil/gas/water flow conditions. *SPE Production & Facilities*, 18(03):170–181, aug 2003.

[26] Andrey Smyshlyaev, Eduardo Cerpa, and Miroslav Krstic. Boundary stabilization of a 1-D wave equation with in-domain antidamping. *SIAM Journal on Control and Optimization*, 48(6):4014–4031, 2010.

[27] Andrey Smyshlyaev and Miroslav Krstic. Closed-form boundary state feedbacks for a class of 1-D partial integro-differential equations. *IEEE Transactions on Automatic Control*, 49(12):2185–2202, 2004.

[28] Andrey Smyshlyaev and Miroslav Krstic. On control design for PDEs with space-dependent diffusivity or time-dependent reactivity. *Automatica*, 41(9):1601–1608, 2005.

[29] Andrey Smyshlyaev and Miroslav Krstic. *Adaptive Control of Parabolic PDEs*. Princeton University Press, 2010.

[30] Timm Strecker and Ole Morten Aamo. Output feedback boundary control of series interconnections of 2 2 semilinear hyperbolic systems. *IFAC-PapersOnLine*, 50(1):663 – 670, 2017. 20th IFAC World Congress.

[31] Gang Tao. *Adaptive Control Design and Analysis*. John Wiley & Sons, Inc., New York, NY, USA, 2003.

[32] Rafael Vazquez, Miroslav Krstic, and Jean-Michel Coron. Backstepping boundary stabilization and state estimation of a 2×2

linear hyperbolic system. In *Proceedings of the 50th IEEE Conference on Decision and Control and European Control Conference*, pages 4937–4942, December 2011.

[33] Jing Zhou, Øyvind Nistad Stamnes, Ole Morten Aamo, and Glenn-Ole Kaasa. Switched control for pressure regulation and kick attenuation in a managed pressure drilling system. *IEEE Transactions on Control Systems Technology*, 19(2):337–350, 2011.

A Proof of Lemma 1 to 4

A.1 Proof of Lemma 1

PROOF. Let

$$V_0(t) = k\frac{1}{2\gamma_1}\tilde{\theta}^2(t) + \frac{1}{2\gamma_2}\tilde{k}^2(t) \tag{A.1}$$

for $t \geq t_F$ where $\tilde{\theta} = \theta - \hat{\theta}$ and $\tilde{k} = k - \hat{k}$. Differentiating with respect to time and inserting (16) yield

$$\begin{aligned}
\dot{V}_0(t) &= -k\frac{1}{\gamma_1}\tilde{\theta}(t)\dot{\hat{\theta}}(t) - \frac{1}{\gamma_2}\tilde{k}(t)\dot{\hat{k}}(t) \\
&= -k\tilde{\theta}(t)\frac{\tilde{e}(t)}{1+y_0^2(t)} - \tilde{k}(t)\left[\hat{\theta}(t) - y_0(t)\right]\frac{\tilde{e}(t)}{1+y_0^2(t)} \\
&= -\frac{\tilde{e}(t)}{1+y_0^2(t)}\left(k\tilde{\theta}(t) + \tilde{k}(t)\left[\hat{\theta}(t) - y_0(t)\right]\right) \\
&= -\frac{\tilde{e}(t)}{1+y_0^2(t)}\left(k\left[\theta - y_0(t)\right] - \hat{k}(t)\left[\hat{\theta}(t) - y_0(t)\right]\right) \\
&= -\frac{\tilde{e}^2(t)}{1+y_0^2(t)} \leq 0
\end{aligned} \tag{A.2}$$

implying $V_0 \in \mathscr{L}_\infty$ and Property 1. Property 2 is trivially guaranteed when using projection. Integrating $\dot{V}_0$ from $t = 0$ to $t = \infty$ yields

$$\int_0^\infty \frac{\tilde{e}^2(\tau)}{1+y_0^2(\tau)}d\tau = V_0(0) - V_0(\infty). \tag{A.3}$$

Since V_0 is a non-increasing function of time and bounded below, $V_0(\infty)$ is finite, and Property 3 follows. From the adaptive law (16a) we immediately see that $\dot{\hat{\theta}} \in \mathscr{L}_2$. For the $\hat{k}$ update law for $t \geq t_F$, we have

$$\dot{\hat{k}}(t) \leq \gamma_2 \left|\frac{\hat{\theta}(t) + y_0(t)}{\sqrt{1+y_0^2(t)}}\right| \left|\frac{\tilde{e}(t)}{\sqrt{1+y_0^2(t)}}\right| \tag{A.4}$$

which shows that also $\dot{\hat{k}} \in \mathscr{L}_2$. Inserting (15) into the adaptive law (16a) yields

$$\dot{\hat{\theta}}(t) = -f(t)\left(k\tilde{\theta}(t) + \tilde{k}(t)\left(\hat{\theta}(t) - y_0(t)\right)\right) \tag{A.5}$$

where $f(t) = \gamma_1/(1+y_0^2(t)) > 0$ for all $t > t_F$. Forming $V_0(t) = \frac{1}{2}\tilde{\theta}^2(t)$, time differentiating and applying Young's inequality to the cross term, we get

$$\begin{aligned}
\dot{V}_0(t) &= -f(t)k\tilde{\theta}^2(t) - \tilde{\theta}(t)f(t)\tilde{k}(t)\left(\hat{\theta}(t) - y_0(t)\right) \\
&\leq -\frac{k}{2}f(t)\tilde{\theta}^2(t) + \frac{1}{2k}f(t)\tilde{k}^2(t)\left(\hat{\theta}(t) - y_0(t)\right)^2.
\end{aligned} \tag{A.6}$$

Since by assumption for Property 5, y_0 is bounded for almost all $t \geq 0$, it follows that $\operatorname{ess\,inf}_{t\geq 0} f(t) > 0$, which along with Property 1 and boundedness of $f(t)$, provide the existence of constants b and $c > 0$ such that

$$\dot{V}_0(t) \leq -c\tilde{\theta}^2(t) + g(t)\tilde{\theta}^2(t) + b\left(\hat{\theta} - y_0(t)\right)^2, \tag{A.7}$$

where $g(t) = 0$ almost everywhere and therefore $g(t) \in \mathscr{L}_1$. Since $(\hat{\theta} - y_0)^2 \in \mathscr{L}_1$, it follows from [18, Lemma D.6] (Lemma 6 in Appendix B) that $V_0 \in \mathscr{L}_1 \cap \mathscr{L}_\infty$ which together with [31, Lemma 2.7] (Lemma 7 in Appendix B) imply $V_0, \tilde{\theta} \to 0$. Convergence in $\hat{k}$ to some constant can be shown by integrating (16b) from $t = 0$ to $T = \infty$ and applying Cauchy-Schwarz' inequality

$$\begin{aligned}
\int_0^T \left|\dot{\hat{k}}(\tau)\right| d\tau \leq \gamma_2 &\sqrt{\int_0^T \left|\hat{\theta}(\tau) - y_0(\tau)\right|^2 d\tau} \\
&\times \sqrt{\int_0^T \left|\frac{\tilde{e}(\tau)}{1+y_0^2(\tau)}\right|^2 d\tau} < \infty
\end{aligned} \tag{A.8}$$

which, by Property 4 and $(\hat{\theta} - y_0)^2 \in \mathscr{L}_1$, shows that $\dot{\hat{k}} \in \mathscr{L}_1$. Then for any $\varepsilon > 0$ there exists a T such that

$$\int_T^\infty \left|\dot{\hat{k}}(\tau)\right| d\tau < \varepsilon. \tag{A.9}$$

Therefore,

$$\left|\hat{k}(t) - \hat{k}(T)\right| \leq \left|\int_T^t \dot{\hat{k}}(\tau)d\tau\right| \leq \int_T^\infty \left|\dot{\hat{k}}(\tau)\right| d\tau < \varepsilon. \tag{A.10}$$

which shows that $\hat{k}(t)$ has a limit as $t \to \infty$ and the second part of the proof of Property 5 is complete.

A.2 Proof of Lemma 2

PROOF. We will in the following use the bounds

$$\sup_{x\in[0,1]} \left|\frac{\partial}{\partial t}\Psi_i(x,t)\right| \leq h_3\mu\left|\dot{\hat{k}}(t)\right|. \tag{A.11}$$

In proving the existence of a solution to the kernel equations (20) in [11], upper bounds on the form $|K^{ij}(x,\xi)| \leq$

$h_1\mu + h_2\mu|\hat{q}(t)|, \{ij\} \in \{uu, uv, vu, vv\}$ are derived. Using the definitions (18) and (23) and differentiating with respect to time yield the upper bound (A.11) for some $h_1, h_2, h_3 > 0$. Solving the reference model (33) along the characteristics for $t \geq t_F$ yields

$$\begin{aligned}\varphi(x,t) =& \lambda^{-1}\int_0^x \Psi_1(\xi, t+\lambda^{-1}(\xi-x))\hat{d}(t+\lambda^{-1}(\xi-x))d\xi \\ &+ \varphi(0, t-\lambda^{-1}x) \qquad \text{(A.12a)}\\ \phi(x,t) =& \mu^{-1}\int_x^1 \Psi_2(\xi, t-\mu^{-1}(\xi-x))\hat{d}(t-\mu^{-1}(\xi-x))d\xi \\ &+ \phi(1, t-\mu^{-1}(1-x)). \qquad \text{(A.12b)}\end{aligned}$$

To simplify the notation let

$$\vartheta(t) = \frac{\hat{d}(t)}{r-\hat{q}(t)}. \qquad \text{(A.13)}$$

Evaluating (A.12) at $x = 0$ and using boundary conditions (33c) and (33d) together with (34) yield

$$\varphi(0,t) = \hat{q}(t)\phi(0,t) + \hat{d}(t) \qquad \text{(A.14)}$$

and

$$\begin{aligned}\phi(0,t) =& \mu^{-1}\int_0^1 \Psi_2(\xi, t-\mu^{-1}\xi)\hat{d}(t-\mu^{-1}\xi)d\xi \\ &+ \tilde{\sigma}\lambda^{-1}\int_0^1 \Psi_1(\xi, t-t_F+\lambda^{-1}\xi)\hat{d}(t-t_F+\lambda^{-1}\xi)d\xi \\ &+ \tilde{\sigma}\varphi(0,t-t_F) + \vartheta(t-\mu^{-1})(1-\tilde{\sigma}r) \\ &- \tilde{\sigma}\lambda^{-1}\int_0^1 \Psi_1(\xi, t-\mu^{-1})\hat{d}(t-\mu^{-1})d\xi \\ &- \mu^{-1}\int_0^1 \Psi_2(\xi, t-\mu^{-1})\hat{d}(t-\mu^{-1})d\xi \\ =& \mu^{-1}\int_0^1\int_{t-\mu^{-1}}^{t-\mu^{-1}\xi} \frac{\partial}{\partial t}\Psi_2(\xi,\tau)\hat{d}(\tau)d\tau d\xi \\ &+ \tilde{\sigma}\lambda^{-1}\int_0^1\int_{t-\mu^{-1}}^{t-t_F+\lambda^{-1}\xi} \frac{\partial}{\partial t}\Psi_1(\xi,\tau)\hat{d}(\tau)d\tau d\xi \\ &+ \tilde{\sigma}\left(\hat{q}(t-t_F)\phi(0,t-t_F) + \hat{d}(t-t_F)\right) \\ &+ \vartheta(t-\mu^{-1})(1-\tilde{\sigma}r). \qquad \text{(A.15)}\end{aligned}$$

Subtracting $\vartheta(t)$ from both sides and grouping similar terms give the following recursion

$$\begin{aligned}&\phi(0,t)-\vartheta(t) \\ &\quad=\mu^{-1}\int_0^1\int_{t-\mu^{-1}}^{t-\mu^{-1}\xi} \frac{d}{d\tau}\Psi_2(\xi,\tau)\hat{d}(\tau)d\tau d\xi \\ &\qquad+\tilde{\sigma}\lambda^{-1}\int_0^1\int_{t-\mu^{-1}}^{t-t_F+\lambda^{-1}\xi} \frac{d}{d\tau}\Psi_1(\xi,\tau)\hat{d}(\tau)d\tau d\xi \\ &\qquad+\tilde{\sigma}\left(\hat{q}(t-t_F)\phi(0,t-t_F)+\hat{d}(t-t_F)\right) \\ &\qquad+\vartheta(t-\mu^{-1})-\vartheta(t)-\tilde{\sigma}r\vartheta(t-\mu^{-1}) \\ &\quad=\mu^{-1}\int_0^1\int_{t-\mu^{-1}}^{t-\mu^{-1}\xi} \frac{d}{d\tau}\Psi_2(\xi,\tau)\hat{d}(\tau)d\tau d\xi \\ &\qquad+\tilde{\sigma}\lambda^{-1}\int_0^1\int_{t-\mu^{-1}}^{t-t_F+\lambda^{-1}\xi} \frac{d}{d\tau}\Psi_1(\xi,\tau)\hat{d}(\tau)d\tau d\xi \\ &\qquad+\tilde{\sigma}\hat{q}(t-t_F)\left(\phi(0,t-t_F)-\vartheta(t-t_F)\right) \\ &\qquad+\vartheta(t-\mu^{-1})-\vartheta(t) \\ &\qquad+\tilde{\sigma}r\vartheta(t-t_F)-\tilde{\sigma}r\vartheta(t-\mu^{-1}) \\ &\quad=\tilde{\sigma}\hat{q}(t-t_F)\left(\phi(0,t-t_F)-\vartheta(t-t_F)\right) \\ &\qquad+\mu^{-1}\int_0^1\int_{t-\mu^{-1}}^{t-\mu^{-1}\xi} \frac{\partial}{\partial t}\Psi_2(\xi,\tau)\hat{d}(\tau)d\tau d\xi \\ &\qquad+\tilde{\sigma}\lambda^{-1}\int_0^1\int_{t-\mu^{-1}}^{t-t_F+\lambda^{-1}\xi} \frac{\partial}{\partial t}\Psi_1(\xi,\tau)\hat{d}(\tau)d\tau d\xi \\ &\qquad-\int_{t-\mu^{-1}}^{t} \frac{d\vartheta(\tau)}{d\tau}d\tau - \tilde{\sigma}r\int_{t-t_F}^{t-\mu^{-1}} \frac{d\vartheta(\tau)}{d\tau}d\tau, \qquad \text{(A.16)}\end{aligned}$$

which, since $|\tilde{\sigma}\hat{q}(t)| \leq |\tilde{\sigma}\max_{t\geq t_F}\hat{q}(t)| < 1$, is stable. By Lemma 1, $\frac{d\vartheta(t)}{dt} = \frac{\dot{\hat{\theta}}}{r-b_0}$ and $\dot{\hat{k}}$ are both bounded and square integrable, implying

$$(\phi(0,\cdot)-\vartheta) \in \mathscr{L}_2 \cap \mathscr{L}_\infty \qquad \text{(A.17)}$$

which from (A.14) is seen to be equivalent to

$$(\varphi(0,\cdot) - r\phi(0,\cdot)) \in \mathscr{L}_2 \cap \mathscr{L}_\infty. \qquad \text{(A.18)}$$

Boundedness in the L_2-norm can be shown using a similar argument.

A.3 Proof of Lemma 3

PROOF.

If $||\varpi|| \in \mathscr{L}_2$ holds, that is

$$\lim_{T\to\infty}\int_0^T\int_0^1 \varpi^2(x,t)dxdt < \infty, \qquad \text{(A.19)}$$

we have after inserting the explicit solution of (38) for $t > \mu^{-1}$

$$\lim_{T\to\infty}\int_{\mu^{-1}}^{T}\int_0^1 \varpi^2(0,t-\mu^{-1}(1-x))dxdt<\infty. \tag{A.20}$$

Substituting $\tau = t-\mu^{-1}(1-x)$ and changing the order of integration yields

$$\lim_{T\to\infty}\left[\int_0^{\mu^{-1}}\int_{\mu^{-1}}^{\tau+\mu^{-1}}+\int_{\mu^{-1}}^{T-\mu^{-1}}\int_{\tau}^{\tau+\mu^{-1}}+\int_{T-\mu^{-1}}^{T}\int_{\tau}^{T}\right] \times\mu\varpi^2(0,\tau)dtd\tau<\infty. \tag{A.21}$$

All the inner integrals evaluate to μ^{-1} or less, and we have

$$\lim_{T\to\infty}\int_0^T \varpi^2(0,\tau)d\tau<\infty. \tag{A.22}$$

That is, $(\nu(0,\cdot)-r\eta(0,\cdot))\in\mathscr{L}_2$. Since

$$\begin{aligned}|e(t)| =&|u(0,t)-rv(0,t)| = |\omega(0,t)-r\zeta(0,t)|\\ \le&|\varpi_1(t)|+|\varphi(0,t)-r\phi(0,t)|\end{aligned} \tag{A.23}$$

and from Lemma 2 that $\varphi(0,t)-r\phi(0,t)\in\mathscr{L}_2\cap\mathscr{L}_\infty$, $e\in\mathscr{L}_2$ follows. $||\varpi||\in\mathscr{L}_\infty$ implies that $\varpi_1(t)$ is bounded a.e, and in turn that e is bounded a.e, which from the definition (14) also implies boundedness of y_0 a.e.

A.4 Proof of Lemma 4

PROOF. Let

$$\varepsilon^2(t) := \frac{\tilde{e}^2(t)}{1+||\varpi||^2} = \frac{\tilde{e}^2(t)}{1+y_0^2(t)}\frac{1+y_0^2(t)}{1+||\varpi||^2}. \tag{A.24}$$

From the definition (14), upper bound $|e(t)|\le|\varpi_1(t)|+|\varphi(0,t)-r\phi(0,t)|$, and the fact that $|\varphi(0,t)-r\phi(0,t)|$ is bounded from Lemma 2, and that $\varpi_1||\varpi||^{-1}$ is bounded a.e., it follows that the fraction $\frac{1+y_0^2}{1+||\varpi||^2}$ is bounded a.e. and since $\frac{\tilde{e}^2}{1+y_0^2}\in\mathscr{L}_1$ from Property 3 in Lemma 1, $\varepsilon\in\mathscr{L}_2$ follows. Let

$$V_1(t) = \lambda^{-1}\int_0^1 e^{-\delta\lambda^{-1}x}\nu^2(x,t)dx \tag{A.25a}$$

$$V_2(t) = \mu^{-1}\int_0^1 e^{\delta\mu^{-1}x}\eta^2(x,t)dx \tag{A.25b}$$

$$V_3(t) = \mu^{-1}\int_0^1 e^{\delta\mu^{-1}x}\varpi^2(x,t)dx, \tag{A.25c}$$

where (ν,η) is given by (37) and ϖ by (38). Differentiating (A.25a), inserting the dynamics (37a), integrating by parts, using boundary condition (37) and substituting in (A.24) give

$$\begin{aligned}\dot{V}_1(t) =&-2\int_0^1 e^{-\delta\lambda^{-1}x}\nu(x,t)\nu_x(x,t)dx,\\ &-2\lambda^{-1}\int_0^1 e^{-\delta\lambda^{-1}x}\nu(x,t)\Psi_1(x,t)\hat{\kappa}(t)\tilde{e}(t)dx,\\ &-2\lambda^{-1}\int_0^1 e^{-\delta\lambda^{-1}x}\nu(x,t)\int_0^x K_t^{uu}(x,\xi,t)\\ &\qquad\times\mathscr{K}_1^{-1}[\nu+\varphi,\eta+\phi](\xi,t)d\xi dx\\ &-2\lambda^{-1}\int_0^1 e^{-\delta\lambda^{-1}x}\nu(x,t)\int_0^x K_t^{uv}(x,\xi,t)\\ &\qquad\times\mathscr{K}_2^{-1}[\nu+\varphi,\eta+\phi](\xi,t)d\xi dx\\ \le&-e^{-\delta\lambda^{-1}}\nu^2(1,t)+(1+\varsigma^{-1})\bar{q}^2\eta^2(0,t)-\delta V_1(t)\\ &+\lambda^{-1}||\Psi_1||^2\bar{\kappa}^2\tilde{e}^2(t)+V_1\\ &+2e^{-\delta\lambda^{-1}}h||K_t^{uu}||^2(V_1(t)+V_2(t)+||\varphi||^2+||\phi||^2)\\ &+2e^{-\delta\lambda^{-1}}h||K_t^{uv}||^2(V_1(t)+V_2(t)+||\varphi||^2+||\phi||^2)\\ &+(1+\varsigma)\bar{\kappa}^2\varepsilon^2(t)+(1+\varsigma)\bar{\kappa}^2\varepsilon^2(t)\mu V_3(t).\end{aligned} \tag{A.26}$$

for some $\varsigma>0$ and where we have defined $\bar{\kappa} := \sup_{t\ge0}\hat{\kappa}(t) = (1+\underline{k})^{-1}$ and used $\sup_{t\ge t_F}\hat{q}^2(t)\le\bar{q}^2$, $\varsigma>0$ and $||\mathscr{K}_i^{-1}[\nu+\varphi,\eta+\phi]||\le h(||\omega||+||\eta||+||\varphi||^2+||\phi||^2)$ for some $h>0$. Differentiating (A.25b) and inserting the dynamics (37b), we get similarly

$$\begin{aligned}\dot{V}_2(t) =&2\int_0^1 e^{\delta\mu^{-1}x}\eta(x,t)\eta_x(x,t)dx,\\ &-2\mu^{-1}\int_0^1 e^{\delta\mu^{-1}x}\eta(x,t)\Psi_2(x,t)\hat{\kappa}(t)\tilde{e}(t)dx,\\ &-2\int_0^1 e^{\delta\mu^{-1}x}\eta(x,t)\int_0^x K_t^{vu}(x,\xi,t)\\ &\qquad\times\mathscr{K}_1^{-1}[\nu+\varphi,\eta+\phi](\xi,t)d\xi dx\\ &-2\int_0^1 e^{\delta\mu^{-1}x}\eta(x,t)\int_0^x K_t^{vv}(x,\xi,t)\\ &\qquad\times\mathscr{K}_2^{-1}[\nu+\varphi,\eta+\phi](\xi,t)d\xi dx\\ \le&e^{\delta\mu^{-1}}\tilde{\sigma}^2\nu^2(1,t)-\eta^2(0)-\delta V_2(t)\\ &+2e^{\delta\mu^{-1}}h||K_t^{vu}||^2(V_1(t)+V_2(t)+||\varphi||^2+||\phi||^2)\\ &+2e^{\delta\mu^{-1}}h||K_t^{vv}||^2(V_1(t)+V_2(t)+||\varphi||^2+||\phi||^2)\\ &+\mu^{-1}e^{\delta\mu^{-1}}||\Psi_2||^2\bar{\kappa}^2\tilde{e}^2(t)+V_2(t).\end{aligned} \tag{A.27}$$

Lastly, differentiating (A.25c), inserting the dynamics (38), and upper bounding $\varpi(0,t)$ by defining $\bar{q}_r := \sup_{t\ge0}2(\hat{q}(t)-r)^2 = 2(r-b_0)^2\bar{\kappa}$, we get

$$\begin{aligned}\dot{V}_3(t) =&2\int_0^1 e^{\delta\mu^{-1}x}\varpi(x,t)\varpi_x(x,t)dx\\ =&e^{\delta\mu^{-1}}\varpi_1^2(t)-\varpi^2(0,t)-\delta V_3(t)\\ \le&e^{\delta\mu^{-1}}(\bar{q}_r\eta^2(0,t)+2\bar{\kappa}^2\varepsilon^2(t)+2\bar{\kappa}^2\varepsilon^2(t)\mu V_3(t))\\ &-\delta V_3(t).\end{aligned} \tag{A.28}$$

Now forming the Lyapunov function candidate

$$V_4(t) = a_1 V_1(t) + a_2 V_2(t) + a_3 V_3(t), \tag{A.29}$$

and defining the integrable functions

$$\begin{aligned} l_1(t) :=& (2 + \varsigma + \lambda^{-1}||\Psi_1||^2 + \mu^{-1} e^{\delta\mu^{-1}}||\Psi_2||^2)\bar{\kappa}^2\varepsilon^2(t) \\ &+ 2e^{-\delta\lambda^{-1}} h(||\varphi||^2 + ||\phi||^2) \\ &\times (||K_t^{uu}||^2 + ||K_t^{uv}||^2 + ||K_t^{vu}||^2 + ||K_t^{vv}||^2) \end{aligned} \tag{A.30a}$$

$$\begin{aligned} l_2(t) :=& (\mu(2 + \varsigma) + ||\Psi_1||^2 + e^{\delta\mu^{-1}}||\Psi_2||^2)\bar{\kappa}^2\varepsilon^2(t) \\ & 2e^{-\delta\lambda^{-1}} h \\ &\times (||K_t^{uu}||^2 + ||K_t^{uv}||^2 + ||K_t^{vu}||^2 + ||K_t^{vv}||^2) \end{aligned} \tag{A.30b}$$

and using $a_3 = a_1 \bar{q}_r^{-1} e^{-\delta\mu^{-1}} \varsigma^{-1}$ gives the upper bound

$$\begin{aligned} V_4(t) \leq& -(\delta - 1)V_4 + l_1(t) + l_2(t)V_4(t) \\ &- (a_1 e^{-\delta\lambda^{-1}} - a_2 e^{\delta\mu^{-1}}\tilde{\sigma}^2)\nu^2(1,t) \\ &- (a_2 - a_1(1 + 2\varsigma^{-1})\bar{q}^2)\eta^2(0,t). \end{aligned} \tag{A.31}$$

Following [9, Theorem 2.4], if $|\tilde{\sigma}\bar{q}| < 1$, we can select $\delta > 1$ and $\varsigma > 0$ such that

$$(e^{\delta(\mu^{-1} + \lambda^{-1})})\tilde{\sigma}^2(1 + 2\varsigma^{-1})\bar{q}^2 < 1 \tag{A.32}$$

and a_1, a_2 such that

$$e^{\delta(\mu^{-1} + \lambda^{-1})}\tilde{\sigma}^2 < \frac{a_1}{a_2} < \frac{1}{(1 + 2\varsigma^{-1})\bar{q}^2} \tag{A.33}$$

obtaining $\dot{V}_4(t) \leq -V_4(t) + l_1(t) + l_2(t)V_4(t)$. It follows from [18, Lemma B.6] that $V_4 \in \mathscr{L}_1 \cap \mathscr{L}_\infty$, and hence (41). Furthermore, from [31, Lemma 2.17] we have that $V_8 \to 0$, which implies (42).

B Additional stability and convergence lemmas

Lemma 6 (Lemma B.6 from [18]) *Let $v(t)$, $l_1(t)$, $l_2(t)$ be real-valued functions defined for $t \geq 0$. Suppose*

$$0 \leq v(t), l_1(t), l_2(t), \ \forall t \geq 0 \tag{B.1a}$$

$$l_1, l_2 \in \mathscr{L}_1 \tag{B.1b}$$

$$\dot{v}(t) \leq -cv(t) + l_1(t)v(t) + l_2(t) \tag{B.1c}$$

for some positive constant c. Then $v \in \mathscr{L}_1 \cap \mathscr{L}_\infty$.

Lemma 7 (Lemma 2.17 from [31]) *Consider a signal g satisfying*

$$\dot{g}(t) = -ag(t) + bh(t) \tag{B.2}$$

for a signal $h \in \mathscr{L}_1$ and some constants $a, b > 0$. Then

$$g \in \mathscr{L}_\infty \tag{B.3}$$

and

$$\lim_{t\to\infty} g(t) = 0. \tag{B.4}$$